



HHS Public Access

Author manuscript

Mol Psychiatry. Author manuscript; available in PMC 2018 November 22.

Published in final edited form as:

Mol Psychiatry. 2018 September ; 23(9): 1–10. doi:10.1038/mp.2017.180.

Corticostriatal circuit defects in *Hoxb8* mutant mice

Naveen Nagarajan^{1,*}, Bryan W. Jones², Peter J. West³, Robert Marc³, and Mario R. Capecchi^{1,*}

¹Howard Hughes Medical Institute, Department of Human Genetics, University of Utah School of Medicine

²Department of Ophthalmology and Visual Sciences, John A. Moran Eye Center, University of Utah School of Medicine

³Department of Pharmacology and Toxicology, University of Utah

Abstract

Hoxb8 mutant mice exhibit compulsive grooming and hair removal dysfunction similar to humans with the OCD-spectrum disorder, trichotillomania. Since, in the mouse brain, the only detectable cells that label with *Hoxb8* cell lineage appear to be microglia, we suggested that defective microglia cause the neuropsychiatric disorder. Does the *Hoxb8* mutation in microglia lead to neural circuit dysfunctions? We demonstrate that *Hoxb8* mutants contain corticostriatal circuit defects. Golgi staining, ultra-structural, and electrophysiological studies of mutants reveal excess dendritic spines, pre- and post-synaptic structural defects, long-term potentiation and miniature postsynaptic current defects. *Hoxb8* mutants also exhibit hyperanxiety and social behavioral deficits similar to mice with neuronal mutations in *Sapap3*, *Slitrk5* and *Shank3*, reported models of OCD and autism spectrum disorders (ASD's). Long-term treatment of *Hoxb8* mutants with fluoxetine, a serotonin reuptake inhibitor (SSRI), reduces excessive grooming, hyperanxiety and social behavioral impairments. These studies provide linkage between the neuronal defects induced by defective *Hoxb8*-microglia, and neuronal dysfunctions directly generated by mutations in synaptic components that result in mice that display similar pathological grooming, hyperanxiety and social impairment deficits. Our results shed light on *Hoxb8* microglia driven circuit-specific defects and therapeutic approaches that will become essential to developing novel therapies for neuropsychiatric diseases such as OCD and ASD's with *Hoxb8*-microglia being the central target.

Introduction

Grooming is an evolutionarily well-conserved innate behavior of rodents and other mammalian species that is essential for survival. The grooming circuit induces hierarchically ordered set of actions, which in *Hoxb8* mutants are characterized by compulsive excessive grooming, hair removal and lesions at the sites of overgrooming^{1–2, 6–7,37}. *Hoxb8* mutant

Users may view, print, copy, and download text and data-mine the content in such documents, for the purposes of academic research, subject always to the full Conditions of use: http://www.nature.com/authors/editorial_policies/license.html#terms

Correspondence: capecchi@genetics.utah.edu; naveen@genetics.utah.edu.

Conflict of Interest The authors declare no conflict of interest.

analysis suggested that defective microglia underlie the behavioral deficits⁷. How *Hoxb8* gene disruption alters neural circuit, induces behavioral dysfunctions and cause neuronal pathology has neither been addressed nor has such ensuing neural damage been previously defined. Functional imaging in humans^{8–9,53} and genetic mutational studies in *SAPAP3*, *Slitrk5* and *Shank3*^{3–5} mutant mice has pointed to corticostriato-thalamo-cortical circuit defects as a basis for OCD-pathogenesis^{10–13,15,22}.

To address the role of *Hoxb8* gene function in neuronal pathology we examined neuronal integrity of *Hoxb8* mutants and evaluated corticostriatal structural and functional synaptic impairments. We further demonstrate that *Hoxb8* mutants exhibit anxiety and social interaction behavioral dysfunction in addition to pathological grooming. These behaviors in mutants are rescued by long-term fluoxetine treatment similar to humans¹⁶. This work ties together *Hoxb8* gene induced neural pathology with the neural *SAPAP3*, *SlitrK5* and *Shank3* mutant^{3–5} mice models of OCD and ASD. We infer that the *Hoxb8* gene in the *Hoxb8* cell lineage normally modulate the corticostriatal circuit and controls grooming behavior. The absence of *Hoxb8* function in microglia leads to aberrant modulation and physical impairment of these neural circuits leading to OCD-like compulsive behavior in mice.

Material and Methods

All experiments were approved by the The Institutional Animal Care and Use Committee (IACUC), University of Utah.

Electron microscopy (EM)

Tissues were fixed (24h) in 1% formaldehyde, 2.5% glutaraldehyde, 3% sucrose, and 1 mM MgSO₄ in 0.1 M cacodylate buffer, osmicated (60 min) in 0.5% OsO₄ in 0.1 M cacodylate buffer, processed in maleate buffer for en bloc staining with uranyl acetate, and processed for resin embedding⁵². 60–90 nm sections were mounted onto Formvar® films and imaged (GATAN Ultrascan 4000) at 80 KeV (JEOL-JEM-1400-EM, 5,000x magnification and nanometer resolution) from 1X1X1 mm³ tissue volume. IR-tools mosaicked TEM data and corrected aberrations and electron-optical distortions after mosaic construction on individual tiles. All statistics used for EM analysis per sample per genotype and grouped analysis is summarized in Supplementary table 2. Sample size for data analysis was determined by power analysis and literature^{3, 5}. Spine and synapse quantification was performed by an experimenter blinded to genotype and the brain region.

Slice electrophysiology

Slices from isolated brains were placed in ice-cold (4°C) oxygenated Sucrose-based Artificial Cerebral Spinal Fluid (ACSF) (95% O₂/5% CO₂) containing (in mM): Sucrose (180.0), KCl (3.0), Na₂PO₄ (1.4), MgSO₄ (3.0), NaHCO₃ (26.0), glucose (10.0), and CaCl₂ (0.5). ACSF contained (in mM): NaCl (126.0), KCl (3.0), Na₂PO₄ (1.4), MgSO₄ (1.0), NaHCO₃ (26.0), glucose (10.0), and CaCl₂ (2.5) (pH 7.3–7.4, 290–300 mOsm).

Corticostratial LTP

Field excitatory post-synaptic potentials (fEPSPs) were recorded (30–31°C) from slices perfused with oxygenated ACSF (2.5 mL/min). Concentric bipolar stimulating electrodes were placed in dorsomedial striatum (DMS) at its interface with corpus callosum^{17–19}. Recording microelectrodes were placed near (250 µm) stimulating electrodes in DMS. fEPSPs were evoked with 100 µs stimuli (1–40 V, stimulation strength 50% of minimal and maximal fEPSP amplitudes).

Whole-cell recordings

Acute brain slices (300 µm thickness) were cut and recovered (45–60 min) in a submerged chamber (31° C) with ACSF (in mM) 125 NaCl, 2.5 KCl, 2.0 CaCl₂, 1 MgCl₂, 1.25 NaH₂PO₄, 25 NaHCO₃ and 15 D-glucose (pH 7.4, 300–310 mOsm) and perfused with oxygenated (95% O₂/5% CO₂) ACSF at 2 ml/min at 31° C. Internal solution was (in mM) 107 CsMeSO₃, 10 CsCl, 3.7 NaCl, 5 TEA-Cl, 20 HEPES, 0.2 EGTA, 5 lidocaine, 4 ATP-magnesium and 0.3 GTP-sodium salt (pH 7.3, 298–301 mOsm). Data were sampled at 10 kHz with low- and high-pass filter set to 1 kHz and 3 Hz. Sample size for data analysis was determined by power analysis and literature. Sample size for all electrophysiological experiments was determined based on the literature^{3–5, 17–20}.

Grooming behavior

Grooming assay used vibration sensitive platforms and laboras software for data analysis. Parameters extracted from grooming assay is shown in Supplementary table 3.

Elevated plus maze, open field and light-dark test

Anxiety was tested in plus maze (5X35X 15X40 cm), open field (40X40X35 cm) and light-dark arena (40X40X35 cm). Mouse movement was tracked using ANY-Maze software. Parameters extracted from anxiety assay are shown in Supplementary table 4.

Three-Chambered social assay

30 minute Social assay was performed in three-chambered compartment. Test mouse was placed in center while intruder mouse in right with left chamber being empty. After placing test mouse at the center for 10-minute habituation, left and right doors were opened for test mouse to interact with empty or intruder chamber. Test mice movements were tracked using Laboras.

Fluoxetine treatment

Mice that underwent fluoxetine or saline treatment were acclimated in home cages for > 7 days. WT and mutants were intraperitoneally injected (5 mg/kg) with fluoxetine once a day for one day, one, five and thirteen weeks. Sample size for all behavioral and drug treatment conditions were determined by literature^{3–5} and power analysis.

All behavioral experiments were conducted blindly with the experimenter blind to genotype and drug treatment conditions.

Results

Hoxb8 mutants show altered pre and postsynaptic structures

We first determined if *Hoxb8* mutants show altered corticostriatal synapse morphology similar to those shown to be defective in SAPAP3 and Slitrk5 mutant mice, well studied mouse models of OCD. We measured dendritic spine density in frontal cortical and striatal neurons using golgi-cox staining. Mutants exhibit significantly higher spine density in frontal cortex but lower density in striatum (Fig. 1a, 1c–1d) implying distinct effects of *Hoxb8* mutation on spine maintenance within cortex and striatum. Spines averaged per mouse reproduced the average value (Supplementary table 1d–1e). To identify the dendritic spine density changes in OCD specific striatal brain regions, as opposed to global spine density changes in the entire striatum, we quantified spine density from dorso and ventro-medial striatum of WT and *Hoxb8* mutants. Spine density in *Hoxb8* mutants increased significantly in both dorso- and ventro-medial striatal regions (Supplementary Fig. 1c, 1e, 1d, 1f) without affecting spine density from visual cortex (Supplementary Fig. 1b, 1g), a control brain region that is independent of OCD circuit. These data suggests that distinct striatal sub-regions show diverse dendritic spine phenotype.

To identify whether the *Hoxb8* mutation affects synaptic structures, we examined asymmetric (excitatory) and symmetric (inhibitory) cortical and striatal synapses using electron microscopy (EM). Representative synapses are displayed and modeled (Fig. 1b, Supplementary Fig. 3a). At asymmetric and symmetric cortical synapses, synaptic length increased significantly compared to WT (Fig. 1e, Supplementary Fig. 2m–2n). Contrastingly, synaptic length decreased significantly at striatal asymmetric and symmetric synapses (Fig. 1f, Supplementary Fig. 2o–2p) suggesting defective but contrasting cortical and striatal structural synapse in mutants. To determine post-synaptic alteration, we quantified postsynaptic density (PSD) length and thickness. PSD length in mutants shifted rightward (Fig. 1g–1h) in cumulative distribution and was significantly longer at asymmetric and symmetric cortical synapses (Fig. 1o). Contrastingly, PSD thickness of asymmetric and symmetric cortical synapses of mutants shifted leftward in cumulative distribution (Fig. 1i–1j) and were significantly smaller than WT (Fig. 1q). Synaptic expansion in mutants concurrently increased pre-synaptic diameter at asymmetric and symmetric synapses, but expanded postsynaptic diameter only at asymmetric synapses (Supplementary Fig. 3b–3e, 3j, 3l, Supplementary table 1). To identify if synaptic structural changes affect active zone, we quantified active zone length and thickness at cortical synapses. Mutants exhibit longer active zones at asymmetric and symmetric synapses (Supplementary-Fig. 2a–2b, 2i, Supplementary Table 1). Changes in the active zone thickness were insignificant at either of the synapses (Supplementary Fig. 2k) although cumulative distribution showed statistical significance for symmetric synapses (Supplementary-Fig. 2d, 2c, Supplementary Table 1). Together the data imply that the *Hoxb8* mutation affects the cortical pre- and post-synapses and results in synaptic expansion at asymmetric and symmetric synapses. Because we detected synaptic expansion within frontal cortical synapses, we asked if such structural alteration result in more or stronger synapses? We analyzed total excitatory and inhibitory synapses within frontal cortex and observed that mutants exhibit significantly increased mono- and total asymmetric but not symmetric synapses (Supplementary Fig. 2q–t)

implying increased synaptic density in mutants in consistence with synaptic structural modification.

In contrast to cortex, *Hoxb8* mutants showed a significant reduction of PSD length (Fig. 1p) and shifted cumulative distribution leftward at asymmetric (Fig. 1k) and symmetric (Fig. 1l) striatal synapses. PSD thickness of asymmetric and symmetric striatal synapses in mutants was significantly greater than WT (Fig. 1r) and shifted cumulative distribution rightward (Fig. 1m–1n). Synaptic contraction concurrently reduced pre and postsynaptic diameter with leftward shifting of cumulative distribution (Supplementary-Fig. 3f–3i, 3k, 3m, Supplementary Table 1). Similar to pre- and postsynaptic contraction, mutants exhibit smaller active zones at asymmetric and symmetric synapses (Supplementary-Fig. 2e–2f, 2j, Supplementary Table 1). Contrast to cortex, active zone thickness shrunk at asymmetric but expanded significantly at symmetric striatal synapses (Supplementary Fig. 2g–2h, 2l, Supplementary Table 1) indicating that *Hoxb8* mutation affects striatal and cortical synapses differentially (Supplementary-Table 1c, Supplementary Table 2). Synaptic analysis revealed a significant increase in mono and total synapses at asymmetric excitatory but reduced mono and total synapses at symmetric synapses (Supplementary Fig. 2u–2x) in mutants consistent with the synaptic structural modification at cortical and striatal synapses in *Hoxb8* mutants leading to an increased excitation at the corticostriatal circuit as has been reported for SAPAP3, Slitrk5 and Shank3 mutant mice^{3–5}.

Altered CNQX-insensitive long-term potentiation and miniature excitatory currents in *Hoxb8* mutants

We investigated whether altered pre- and postsynaptic structure observed in frontal cortex and striatum affected corticostriatal neurotransmission in *Hoxb8* mutants. The input-output (IO) curves, slope normalized to peak response, field potential amplitudes and paired-pulse ratio at striatal synapses revealed insignificant difference between mutant and WT slices (Supplementary Fig. 4a–4c, Fig. 2a) in response to layer 5/6 cortical fiber stimulation implying that the electrophysiological properties and short-term plasticity is intact in mutants.

To probe presynaptic plasticity, population spike responses were measured in dorsal striatum. Single pulse layer 5/6 cortical stimulation evoked a population spike that was dependent on synaptic glutamate release and postsynaptic α -amino-3-hydroxy-5-methyl-4-isoxazolepropionic acid receptor (AMPA)/kainate receptors¹⁷. Population spike consisted of non-synaptic (S1, source current) presynaptic component and synaptically mediated postsynaptic component (S2, sink current)^{17–19, 23} (Fig. 2b–2c). Because of non-laminar striatal organization, sink and source currents a) overlap in space b) arise from action potentials with shorter latency c) are- CNQX-insensitive and interchangeable measures of presynaptic depolarization.

In control experiments, CNQX, (AMPA/kainate receptor antagonist) blocked the S2 but not S1 component (Fig. 2b) indicating that the action potential dependent component is CNQX-sensitive (S2), while the independent component is CNQX-insensitive (S1). To investigate whether mutants show changes in S2 versus S1, tetanic stimulation was applied to DMS and LTP was measured. Strikingly, the S1 increased significantly in mutants compared to WT

(Fig. 2d) without affecting the S2 (Fig. 2e) suggesting that the loss of the *Hoxb8* gene affects CNQX-independent (cortical driven) but not CNQX-dependent (intra-striatal) LTP. S1 versus S2 field potential amplitudes did not differ significantly (Supplementary Fig. 4d) implying that the postsynaptic striatal output is smaller despite presynaptic changes consistent with the reduced spine density, synapse and PSD length of mutants (Fig. 1d, 1f, 1p) at striatal synapses analyzed.

Because cortical and striatal spine density and PSD morphology was altered, we questioned if electrophysiological signature of such synaptic change exist in DMS. We recorded AMPA-receptor mediated excitatory miniature evoked postsynaptic currents (mEPSCs) from dorsal MSNs. Two distinct mEPSC types were detected in MSNs of mutants that were distinguishable by response kinetics and decay time and categorized into slow (Group 1) and fast (Group 2) miniature events (Fig. 2g–2h, Supplementary Fig. 4f). Representative events are displayed in Fig. 2h. Group 1 MSNs of mutants exhibit significantly longer inter-event interval (IEI) with higher amplitudes (Fig. 2g, 2i, 2k) while group 2 MSNs showed significantly reduced IEI and mEPSC amplitudes relative to WT mice (Fig. 2g, 2j, 2l) implying that the probability of the presynaptic neurotransmitter release and postsynaptic AMPA receptors might be affected in opposite way. These effects were prominent when rise and decay times (Supplementary Fig. 4g–j), mEPSC charge, event half-width (Supplementary Fig. 4k–n) and frequency (Supplementary Fig. 5a–5b) were analyzed. The relationship between a) mEPSC amplitude and 10–90% rise time (Supplementary Fig. 5c–5d), b) amplitude and average rise rate (Supplementary Fig. 5e–5f), and c) event half width and 10–90% rise time (Supplementary Fig. 5g–5h), were distinguishable between WT and mutants. These data imply that mEPSC events of MSNs are affected in mutants at single neuronal level.

***Hoxb8* mutants show impaired grooming, anxiety and social behaviors**

To determine the role of *Hoxb8* mutation in grooming, we used 24-hour automatic laboras platform containing sensitive vibration detectors to detect grooming and non-grooming behaviors²⁰. Reproducibly^{6,7}, laboras detected significantly higher self-grooming behavior in mutants compared to WT mice (Fig. 3a, Supplementary Table 3–4).

Two features common to OCD and ASD, are hyperanxiety and social behavioral deficits^{3–5,13}. We investigated whether such behaviors in mutants are altered. In plus maze test, mutants spent significantly more time in closed arm compared to WT mice (Fig 3b–3c) without altering distance in closed arm (Supplementary Fig. 6a) implying that mutants are more anxious in plus maze. Mutants spent significantly decreased time in open arm under different light intensities (1.7 fold at 75 lx, 2.7 fold at 100 lx; Supplementary Fig. 6b), traveled for shorter distances (1.5 fold, 75 lx; 3.2 fold, 100 lx; Supplementary Fig. 6c) and had longer latencies (3.7 fold, 75 lx; 4.9 fold, 100 lx; Supplementary Fig. 6d) than controls.

In open field test, an additional indicator of anxiety level, mutants exhibit significantly reduced- time at the center (Fig. 3d–3e), line crossings, entries and circling numbers (Supplementary Fig. 6f–6e) implying higher anxiety levels relative to controls. Both male and female mutants showed higher anxiety levels (Supplementary Table 5). In light-dark test, mutants spent reduced time in light (Fig. 3f) and more time in dark chamber

(Supplementary Fig. 6h) compared to WT mice without affecting the total light zone entries (Supplementary Fig. 6i). All these anxiety tests suggested that *Hoxb8* mutants exhibit hyperanxiety levels relative to controls.

We tested social behaviors in *Hoxb8* mutants using a three-chambered social assay in which the test subject (WT or mutant, male or female) is placed at the center, with an empty left chamber and an intruder mouse in the right chamber. Mutants spent significantly reduced time socially interacting with the intruder (Fig. 3h). Heat maps derived from male and female mutants (Fig. 3g) during social assay show evidence that female mutants exhibit significantly higher social impairment compared to males. To determine whether mutants interact normally with cage-mates, test mice were challenged to interact with a cage-mate in social assay. Mutants showed a significant social deficit even with a cage-mate, a defect that was confined to the female mutants (Fig. 3i, Supplementary Fig. 6j) indicating that female mutants show higher detectable social impairment than males.

Fluoxetine treatment of *Hoxb8* mutants alleviates grooming, anxiety and social impairment behaviors

We evaluated whether fluoxetine ameliorates behavioral abnormalities in *Hoxb8* mutants. One week, but not one-day treatment reduced grooming time of mutants without significantly affecting the WT mice (Supplementary Fig. 7a). No sedative effect was detected as measured by locomotion and immobility between saline or fluoxetine-treated groups, implying the appropriateness of drug dosage (Fig. 4b–4c). To determine long-term effects of fluoxetine on anxiety, mutants and WT mice were chronically treated for five weeks. In plus maze test, treated mutants spent a 3.4 fold increased time in open-arm compared to saline-treated mutants (Fig. 4d). Treated mutants that spent more time at the center of the open field compared to saline treated mutants did not reach WT-levels (Fig. 4e) implying a partial rescue. When exposed to a novel intruder, treated mutants compared to WT mice spent a reduced time in empty chamber and similar time at the center or with the intruder mouse (Fig. 4g–4h) implying that the treatment resulted in improved social behaviors. To investigate if the alleviated behaviors are sustained during chronic fluoxetine treatment, mutants and WT mice were treated with fluoxetine upto thirteen weeks. Anxiety and exploratory locomotion were tested using light-dark and open field tests. The distance at the center or periphery of open field (Supplementary Fig. 7b–7c) and the time in light zone (Supplementary Fig. 7d) reached WT-like levels implying extensive rescue. Amount of time spent by mutants in light zone during light-dark exploration increased to WT-levels (Fig. 4f). These data demonstrate that fluoxetine treatment alleviates pathological grooming, anxiety and aberrant social behaviors in *Hoxb8* mutants.

Discussion

Targeted disruption of *Hoxb8* gene causes brain specific^{6,7} compulsive hair removal behavior closely resembling the OCD spectrum disorder Trichotillomania in humans²¹. We now show that *Hoxb8* loss of function results in synaptic and physiological defects within cortico-striatal circuit. This CS defect in mutants resulted in frontal cortical synaptic expansion and striatal synaptic contraction. The increased cortical synapse and spine density

within frontal cortex in conjunction with increased dendritic spines in dorso- and ventro-medial sub-regions of striatum implicate a potential increase in excitatory corticostriatal synapse.

These synaptic modifications were also detectable electrophysiologically. At circuit level we detected impaired CNQX independent striatal synaptic LTP. This plasticity may emerge from changes in presynaptic mPFC neurons synapsing onto striatal mSNs during action potential firing at frequencies that induce synaptic plasticity. mEPSC recordings from individual mSNs showed two distinct mEPSCs, higher amplitude, low-frequency and longer IEI (group 1) and the lower amplitude, high-frequency and reduced IEI (group 2) implying the sensitivity of whole-cell recordings to measure synaptic properties of MSNs.

Mutants exhibit grooming, anxiety and social behavioral impairment. Fluoxetine alleviates grooming, anxiety and social deficits in mutants similar to *Sapap3*, *Slitrk5* and *Shank3* based OCD/ASD mouse models and human OCD patients^{9,34,14,24–25,35–36,50–51}.

A direct correlation of immune dysfunction and neuropsychiatric disorders is observed in major depression, OCD, Autism, Schizophrenia and Alzheimer's disease^{38–49}. Consequences of *Hoxb8* gene deficiency that results in corticostriatal synaptic aberration provides an independent way that brain appear to utilize to mediate and modulate repetitive behaviors. Interestingly, the loss of *Hoxb8* gene function that results in excessive grooming behavior was not restricted to repetitive behaviors since we detected fluoxetine-sensitive hyperanxiety and social behavioral deficit in *Hoxb8* mutants similar to trichotillomania-type OCD patients^{26–27, 49–51}.

Although the causative agents of the neuropsychiatric disorder in *Hoxb8*-mutant mice versus *Sapap3*, *Slitrk5*, and *Shank3* mutant mice are very different, defective microglia versus defective synaptic components, the end results, both in terms of behavioral deficits, including high levels of anxiety and the affected neural circuits, the corticostriatal interface, are very similar. These results strongly support the hypothesis that in the absence of proper maintenance of circuit modulation by *Hoxb8*-microglia, very similar neural circuit damage ensues in *Hoxb8*, *Sapap3*, *Slitrk5* and *Shank3* mutant mice, resulting in very similar behavioral pathology.

Hoxb8 gene thus appears to play an important role in maintaining brain homeostasis in regulating corticostriatal circuit function and behavioral output. *Hoxb8* gene dysfunction would alter synaptic morphology and physiological properties and thereby affect behaviors, the output of which would depend on the constellation of genetic and environmental insults pertinent to individual patient. Such models tie together immune dysfunctions, particularly pertaining to *Hoxb8* gene function through microglia^{28–34}, the brain's immune system, with repetitive and anxiety behaviors and a spectrum of neuropsychiatric disorders.

Supplementary Material

Refer to Web version on PubMed Central for supplementary material.

Acknowledgments

We would like to thank A. Boulet and K. Higgins for insightful discussions on the manuscript and editing. S.K. Chen for experimental discussion; H. Elderling, Metris for technical support, Shotaro Matsuoka for genotyping, A. Gosdis, and V. Krishnegowda for their participation in early experiments. This work was supported by Seed grant and research instrumentation funding from University of Utah to N.N and M.R.C, HHMI, NIH/NEI, EY02576-36, EY015128-8 and EY014800-08 (P30) to B.W.J and R.M.

References

1. Sachs BD. The development of grooming and its expression in adult animals. *Ann. N. Y. Acad. Sci.* 1988; 525:1–17.
2. Graybiel AM, Saka E. A genetic basis for obsessive grooming. *Neuron.* 2002; 33(1):1–2. [PubMed: 11779470]
3. Welch JM, Lu J, Rodriguiz RM, Trotta NC, Peca J, Ding JD, et al. Cortico-striatal synaptic defects and OCD-like behaviours in Sapap3-mutants. *Nature.* 2007; 448:894–900. [PubMed: 17713528]
4. Shmelkov SV, Hormigo A, Jing D, Proenca CC, Bath KG, Milde T, et al. Slitrk5 deficiency impairs corticostriatal circuitry and leads to obsessive-compulsive-like behaviours in mice. *Nature medicine.* 2010; 16:598–602.
5. Peca J, Feliciano C, Ting JT, Wang W, Wells MF, Venkatraman TN, et al. Shank3 mutants display autistic-like behaviours and striatal dysfunction. *Nature.* 2011; 472:437–442. [PubMed: 21423165]
6. Greer JM, Capecchi MR. Hoxb8 is required for normal grooming behaviour in mice. *Neuron.* 2002; 33:23–34. [PubMed: 11779477]
7. Chen SK, Tvrdik P, Peden E, Cho S, Wu S, Spangrude G, et al. Hematopoietic origin of pathological grooming in Hoxb8 mutants. *Cell.* 2010; 141:775–785. [PubMed: 20510925]
8. Graybiel AM. Habits, rituals, and the evaluative brain. *Annual review of neuroscience.* 2008; 31:359–387.
9. Fineberg NA, Chamberlain SR, Hollander E, Boulougouris V, Robbins TW. Translational approaches to obsessive-compulsive disorder: from animal models to clinical treatment. *British journal of pharmacology.* 2011; 164:1044–1061. [PubMed: 21486280]
10. Menzies L, Chamberlain SR, Laird AR, Thelen SM, Sahakian BJ, Bullmore ET. Integrating evidence from neuroimaging and neuropsychological studies of obsessive-compulsive disorder: the orbitofronto-striatal model revisited. *Neuroscience and biobehavioural reviews.* 2008; 32:525–549.
11. Beucke JC, Sepulcre J, Talukdar T, Linnman C, Zschenderlein K, Endrass T, Kaufmann C, Kathmann N. (2013). Abnormally high degree connectivity of the orbitofrontal cortex in obsessive-compulsive disorder. *JAMA Psychiatry.* 2013; 70(6):619–29. [PubMed: 23740050]
12. Ahmari SE, Spellman T, Douglass NL, Kheirbek MA, Simpson HB, Deisseroth K, et al. Repeated cortico-striatal stimulation generates persistent OCD-like behaviour. *Science.* 2013; 340:1234–1239. [PubMed: 23744948]
13. Schmeisser MJ, Ey E, Wegener S, Bockmann J, Stempel AV, Kuebler A, et al. Autistic-like behaviours and hyperactivity in mice lacking ProSAP1/Shank2. *Nature.* 2012; 486:256–260. [PubMed: 22699619]
14. Krebs G, Heyman I. Obsessive-compulsive disorder in children and adolescents. *Archives of disease in childhood.* 2014; doi: 10.1136/archdischild-2014-306934
15. Shepherd GM. Corticostriatal connectivity and its role in disease. *Nature reviews. Neuroscience.* 2013; 14:278–291. [PubMed: 23511908]
16. Geller DA, Hoog SL, Heiligenstein JH, Ricardi RK, Tamura R, Kluszynski S, et al. Fluoxetine treatment for obsessive-compulsive disorder in children and adolescents: a placebo-controlled clinical trial. *Journal of the American Academy of Child and Adolescent Psychiatry.* 2001; 40:773–779. [PubMed: 11437015]
17. Chen YH, Harvey BK, Hoffman AF, Wang Y, Chiang YH, Lupica CR. MPTP-induced deficits in striatal synaptic plasticity are prevented by glial cell line-derived neurotrophic factor expressed via an adeno-associated viral vector. *FASEB journal: official publication of the Federation of American Societies for Experimental Biology.* 2008; 22:261–275. [PubMed: 17690153]

18. Cordingley GE, Weight FF. Non-cholinergic synaptic excitation in neostriatum: pharmacological evidence for mediation by a glutamate-like transmitter. *British journal of pharmacology*. 1986; 88:847–856. [PubMed: 2874861]
19. Malenka RC, Kocsis JD. Presynaptic actions of carbachol and adenosine on corticostriatal synaptic transmission studied in vitro. *The Journal of neuroscience: the official journal of the Society for Neuroscience*. 1988; 8:3750–3756. [PubMed: 2848109]
20. Quinn LP, Stean TO, Chapman H, Brown M, Vidgeon-Hart M, Upton N, et al. Further validation of LABORAS using various dopaminergic manipulations in mice including MPTP-induced nigro-striatal degeneration. *Journal of neuroscience methods*. 2006; 156:218–227. [PubMed: 16626808]
21. Diefenbach GJ, Tolin DF, Hannan S, Crocetto J, Worhunsky P. Trichotillomania: impact on psychosocial functioning and quality of life. *Behaviour research and therapy*. 2005; 43:869–884. [PubMed: 15896284]
22. Burguiere E, Monteiro P, Feng G, Graybiel AM. Optogenetic stimulation of lateral orbitofronto-striatal pathway suppresses compulsive behaviours. *Science*. 2013; 340:1243–1246. [PubMed: 23744950]
23. Chen YH, Harvey BK, Hoffman AF, Wang Y, Chiang YH, Lupica CR. MPTP-induced deficits in striatal synaptic plasticity are prevented by glial cell line-derived neurotrophic factor expressed via an adeno-associated viral vector. *FASEB J*. 2008; 22(1):261–75. [PubMed: 17690153]
24. Gkogkas CG, Khoutorsky A, Ran I, Rampakakis E, Nevarko T, Weatherill DB, et al. Autism-related deficits via dysregulated eIF4E-dependent translational control. *Nature*. 2013; 493:371–377. [PubMed: 23172145]
25. Han S, Tai C, Westenbroek RE, Yu FH, Cheah CS, Potter GB, et al. Autistic-like behaviour in *Scn1a*+/- mice and rescue by enhanced GABA-mediated neurotransmission. *Nature*. 2012; 489:385–390. [PubMed: 22914087]
26. Sakai Y, Narumoto J, Nishida S, Nakamae T, Yamada K, Nishimura T, et al. Corticostriatal functional connectivity in non-medicated patients with obsessive-compulsive disorder. *European psychiatry: the journal of the Association of European Psychiatrists*. 2011; 26:463–469. [PubMed: 21067900]
27. Harrison BJ, Soriano-Mas C, Pujol J, Ortiz H, López-Solà M, Hernández-Ribas R, et al. Altered corticostriatal functional connectivity in obsessive-compulsive disorder. *Archives of general psychiatry*. 2009; 66:1189–1200. [PubMed: 19884607]
28. Ransohoff RM, Liu L, Cardona AE. Chemokines and chemokine receptors: multipurpose players in neuroinflammation. *Int. Rev. Neurobiol*. 2007; 82:187–204. [PubMed: 17678962]
29. Stevens B, Allen NJ, Vazquez LE, Howell GR, Christopherson KS, Nouri N, et al. The classical complement cascade mediates CNS synapse elimination. *Cell*. 2007; 131(6):1164–78. [PubMed: 18083105]
30. Ransohoff RM, Cardona AE. The myeloid cells of the central nervous system parenchyma. *Nature*. 2010; 468(7321):253–62. [PubMed: 21068834]
31. Paolicelli RC, Bolasco G, Pagani F, Maggi L, Scianni M, Panzanelli P, et al. Synaptic pruning by microglia is necessary for normal brain development. *Science*. 2011; 333(6048):1456–1458. [PubMed: 21778362]
32. Prinz M, Priller J, Sisodia SS, Ransohoff RM. Heterogeneity of CNS myeloid cells and their roles in neurodegeneration. *Nature Neuroscience*. 2011; 14(10):1227–35. [PubMed: 21952260]
33. Schafer DP, Lehrman EK, Kautzman AG, Koyama R, Mardinly AR, Yamasaki R, et al. Microglia sculpt postnatal neural circuits in an activity and complement-dependent manner. *Neuron*. 2012; 74(4):691–705. [PubMed: 22632727]
34. Frick LR, Williams K, Pittenger C. Microglial dysregulation in psychiatric disease. *Clinical and developmental immunology*. 2013:608654. [PubMed: 23690824]
35. Moore ML, Eichner SF, Jones JR. Treating functional impairment of autism with selective serotonin-reuptake inhibitors. *The Annals of pharmacotherapy*. 2004; 38:1515–1519. [PubMed: 15292500]
36. Hollander E, Phillips A, Chaplin W, Zagursky K, Novotny S, Wasserman S, et al. A placebo controlled crossover trial of liquid fluoxetine on repetitive behaviours in childhood and adolescent

- autism. *Neuropsychopharmacology: official publication of the American College of Neuropsychopharmacology*. 2005; 30:582–589. [PubMed: 15602505]
37. Graybiel AM, Rauch SL. Toward a neurobiology of obsessive-compulsive disorder. *Neuron*. 2000; 28:343–347. [PubMed: 11144344]
38. Ashwood P, Wills S, Van de Water J. The immune response in autism: a new frontier for autism research. *J Leukoc Biol*. 2005; 80:1–15.
39. Da Rocha FF, Correa H, Teixeira AL. Obsessive-compulsive disorder and immunology: a review. *Prog Neuropsychopharmacol Biol Psychiatry*. 2008; 32:1139–1146. [PubMed: 18262706]
40. Kronfol Z, Remick DG. Cytokines and the brain: implications for clinical psychiatry. *Am J Psychiatry*. 2000; 157:683–694. [PubMed: 10784457]
41. Lang UE, Puls I, Muller DJ, Strutz-Seebohm N, Gallinat J. Molecular mechanisms of schizophrenia. *Cell Physiol Biochem*. 2007; 20:687–702. [PubMed: 17982252]
42. Leonard BE, Myint A. The psychoneuroimmunology of depression. *Hum Psychopharmacol*. 2009; 24:165–175. [PubMed: 19212943]
43. Strous RD, Shoenfeld Y. Schizophrenia, autoimmunity and immune system dysregulation: a comprehensive model updated and revisited. *J Autoimmun*. 2006; 27(2):71–80. [PubMed: 16997531]
44. Hounie AG, Cappi C, Cordeiro Q, Sampaio AS, Moraes I, Rosario MC, et al. TNF-alpha polymorphisms are associated with obsessive-compulsive disorder. *Neurosci Lett*. 2008; 442:86–90. [PubMed: 18639610]
45. Purcell SM, Wray NR, Stone JL, Visscher PM, O'Donovan MC, Sullivan PF, et al. Common polygenic variation contributes to risk of schizophrenia and bipolar disorder. *Nature*. 2009; 460:748–752. [PubMed: 19571811]
46. Shi J, Levinson DF, Duan J, Sanders AR, Zheng Y, Pe'er I, Dudbridge F, Holmans PA, Whittemore AS, Mowry BJ, et al. Common variants on chromosome 6p22.1 are associated with schizophrenia. *Nature*. 2009; 460:753–757. [PubMed: 19571809]
47. Stefansson H, Ophoff RA, Steinberg S, Andreassen OA, Cichon S, Rujescu D, Werge T, Pietilainen OP, Mors O, Mortensen PB, et al. Common variants conferring risk of schizophrenia. *Nature*. 2009; 460:744–747. [PubMed: 19571808]
48. Luthi A, Lüscher C. Pathological circuit function underlying addiction and anxiety disorders. *Nature Neuroscience*. 2014; 12:1635–43.
49. Markarian Y, Larson MJ, Aldea MA, Good D, Berkeljon A, Murphy TK, et al. Multiple pathways to functional impairment in obsessive-compulsive disorder. *Clin Psychol Rev*. 2010; 30(1):78–88. [PubMed: 19853982]
50. Koran LM, Ringold A, Hewlett W. Fluoxetine for trichotillomania: an open clinical trial. *Psychopharmacol Bull*. 1992; 28(2):145–149. [PubMed: 1513916]
51. Rossi A, Barraco A, Donda P. Fluoxetine: a review on evidence based medicine. *Ann. Gen. Hosp. Psychiatry*. 2004; 3(1):2. [PubMed: 14962351]
52. Marc RE, Liu W. Fundamental GABAergic amacrine cell circuitries in the retina: nested feedback, concatenated inhibition, and axosomatic synapses. *J Comp Neurol*. 2000; 425:560–582. [PubMed: 10975880]
53. Di Martino A, Kelly C, Grzadzinski R, Zuo XN, Mennes M, Mairena MA, et al. Aberrant striatal functional connectivity in children with autism. *Biological psychiatry*. 2011; 69:847–856. [PubMed: 21195388]
54. Anderson JR, Jones BW, Yang JH, Shaw MV, Watt CB, Koshevoy P, et al. A computational framework for ultrastructural mapping of neural circuitry. *PLoS biology*. 2009; 7:e1000074. [PubMed: 19855814]

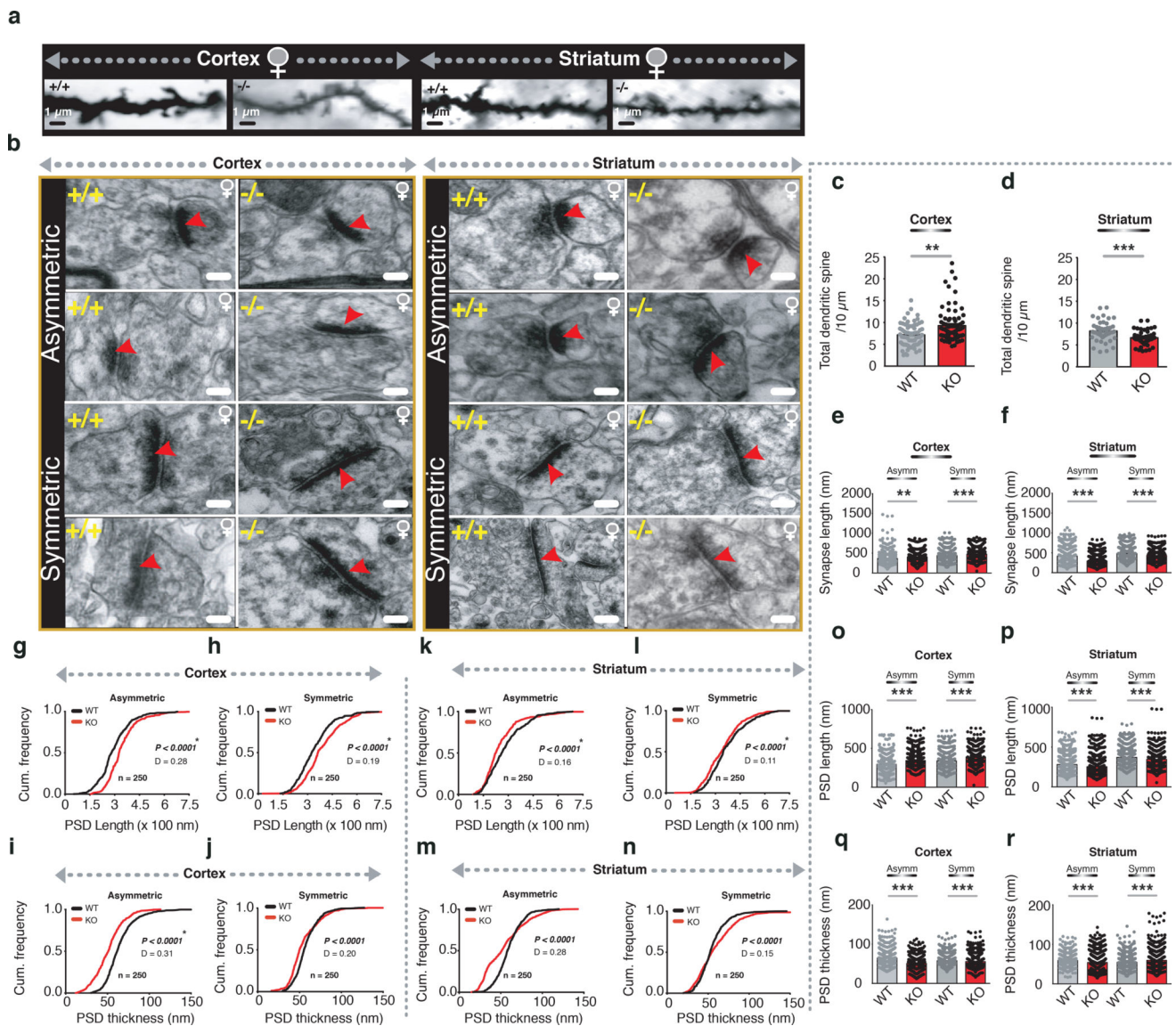


Figure 1. Altered cortical and striatal synapses in *Hoxb8* mutants

a) Representative dendritic spines from 6 months old WT and *Hoxb8* female mutant mice from frontal cortical and dorsal striatal regions. Scale bar: 1 μ m. **b)** Representative electron microscopic images of cortical-asymmetric, cortical-symmetric, striatal-asymmetric and striatal-symmetric synapses from 6 months old WT and *Hoxb8* mutant brains and visualized using Viking software^{52, 54}. Scale bar: 100 nm **c, d)** Significantly increased cortical ($P=0.0034$, $F=9.118$, 28 WT and 29 mutant neurons, 2–3 healthy dendrites per neuron) (c) but decreased (d) striatal spine density ($P=0.001$, $F=10.488$, 13 WT and 18 mutant neurons, 2–3 healthy dendrites per neuron) in female *Hoxb8* mutants (3 litters per group, 8 months old mice) using golgi staining (Fd Neurotechnologies inc). ‘n’ represents the total dendrites analyzed per genotype per brain region. **e, f)** Bar plot displaying significantly increased synapse length at cortical asymmetric ($P=0.00012$, $F=14.8310$) and symmetric ($P<0.0001$, $F=19.8205$) (e) but a significantly decreased striatal asymmetric ($P<0.0001$, $F=138.0321$) and symmetric synapses ($P<0.0001$, $F=37.9242$) (f). **(g–j)** Cumulative probability plot

demonstrating a significant rightward shift in the PSD length in *Hoxb8* mutants compared to WT mice (g, $P<0.0001$, $D=0.2815$; h, $P<0.0001$, $D=0.1992$) but a significant leftward shift in PSD thickness for cortical asymmetric and cortical symmetric synapses (i, $P<0.0001$, $D=0.3187$; j, $P<0.0001$, $D=0.2045$). **(k–n)** A contrasting significant decrease (leftward shift) within striatal-asymmetric (k, $P<0.0001$, $D=0.1595$) and symmetric (l, $P<0.0001$, $D=0.1156$) synapses for PSD length and PSD thickness (m, $P<0.0001$, $D=0.28$; n, $P<0.0001$, $D=0.15$). **(o–p)** Bar graph representation of significantly increased PSD length at cortical-asymmetric ($P<0.0001$, $F=93.2869$) and cortical-symmetric ($P<0.0001$, $F=53.6979$) (o) synapses of *Hoxb8* mutants but a contrasting decrease within striatal-asymmetric (p) ($P<0.0001$, $F=22.1849$) and striatal-symmetric synapses (p) ($P<0.0001$, $F=18.1742$). **(q–r)** Bar graph representation of significantly decreased PSD thickness at cortical-asymmetric ($P<0.0001$, $F=192.3888$) and cortical-symmetric ($P=0.014$, $F=5.9328$) (q) synapses of *Hoxb8* mutants but a contrasting increase within striatal-asymmetric ($P<0.0001$, $F=30.8782$) and striatal-symmetric ($P<0.0001$, $F=17.4861$) (r) synapses. Red arrow represents post-synaptic density in individual synapse. All analysis was conducted on WT and *Hoxb8* mutant female mice brains. One-way ANOVA and Tukey's posthoc test (**c–f**, **o–r**). Kolmogorov-Smirnov test, (**g–n**).

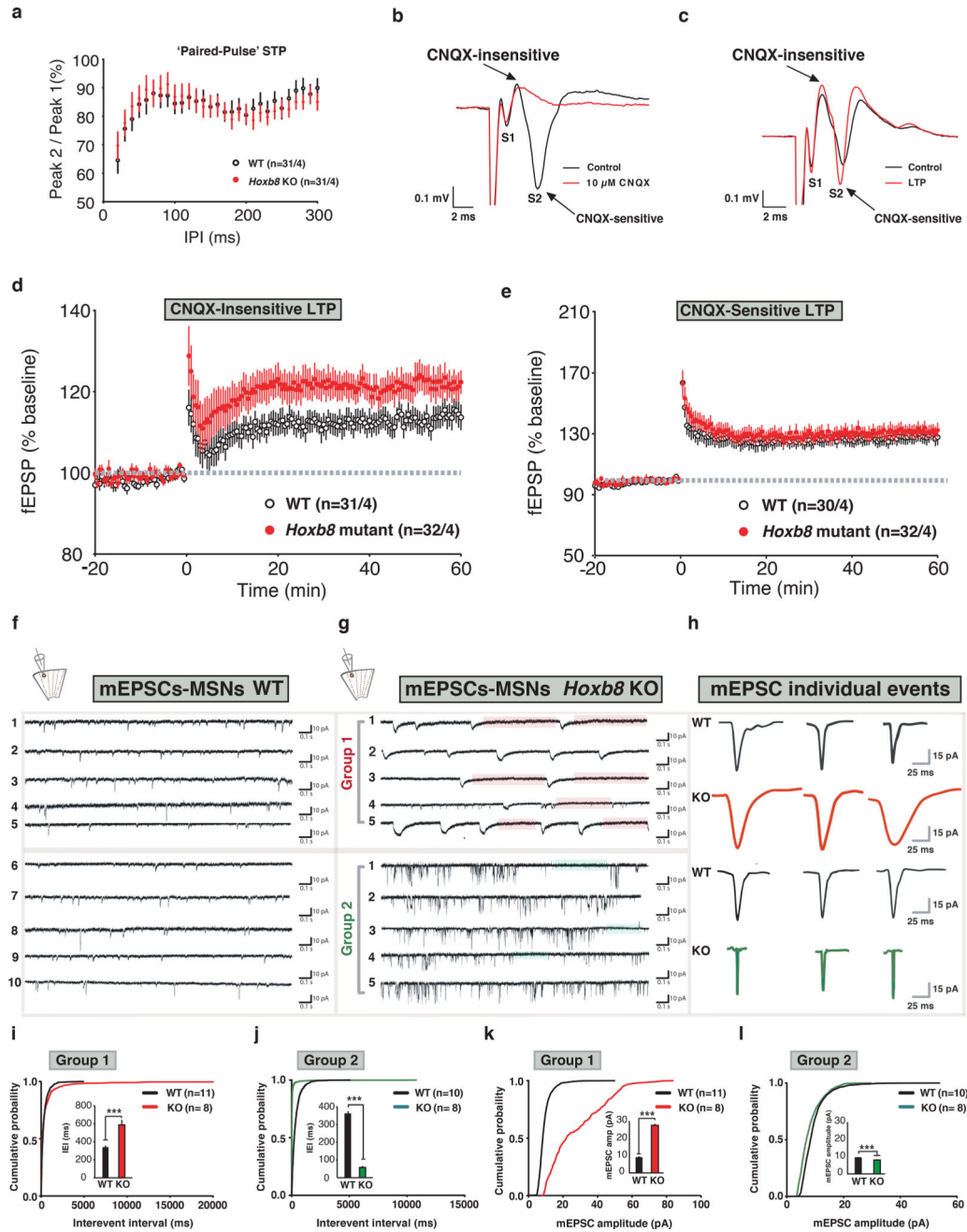


Figure 2. Altered CNQX independent form of LTP and miniature EPSCs in *Hoxb8* mutants at corticostriatal synapses

a) Paired-pulse ratio is unchanged in mutants ($P=0.3453$, $F(28, 1680)=1.086$ for interaction; $P<0.0001$, $F(28,1680)=10.09$ for interpulse interval, $P=0.9560$, $F(1, 60)=0.003074$ for genotype; $P<0.0001$, $F(60,1680)=76.89$ for subjects matching). Paired-pulse ratio of the fEPSP amplitudes was assessed using inter-pulse intervals between 20–300 ms in 10 ms intervals. Single stimuli were given to slices every 30 s for a 30 min to collect baseline. Representative traces and measurements are the average from five consecutive traces. **b)** Representative trace of field potentials in \pm CNQX condition (black and red trace). S1, non-synaptic and S2, synaptically mediated component. Overlaid traces show the sensitivity of

S1 and S2 component to CNQX. **c**) Overlaid trace of field potential recording under control (black) and LTP (red) condition showing S1 and S2 components. Scale bar, 0.1mV (Y-axis) and 2 ms (X-axis). **d**) Increased CNQX-insensitive LTP for WT (black) and mutants (red) ($P=0.1665$, $F(60, 3300)=1.177$ for interaction; $P=0.0014$, $F(60, 3300)=1.642$ for interpulse interval, $P=0.0378$, $F(1, 55)=4.531$ for genotype; $P<0.0001$, $F(55, 3300) = 524.5$ for matched subjects). LTP was induced by high frequency stimulation (1 second/100 Hz). Low frequency stimulation was resumed for 60 min to quantify LTP relative to baseline. **e**) Normal CNQX-sensitive LTP for WT (black) and mutants (red) ($P=0.9477$, $F(60, 3060)=0.7213$ for interaction; $P=0.0316$, $F(60, 3060)=1.371$ for time; $P=0.558$, $F(1, 51)=0.3471$ for genotype and $P<0.0001$, $F(51, 3060)=476.7$ for matched subjects, Two-way ANOVA repeated measures). Significance was determined at $P<0.05$. Data were excluded if the slope of fEPSPs during the 30 min baseline changed by $>20\%$. **f, g**) AMPA receptor mediated mEPSC recording traces at -70 mV from dorsomedial striatal MSNs from parasagittal corticostriatal acute brain slices for WT (left) and *Hoxb8* mutants ($n=3$ mice per genotype, 3 week old) isolated in the presence of TTX ($1 \mu\text{M}$), DL-2-amino-5-phosphonovaleric acid ($50 \mu\text{M}$), D-Serine ($10 \mu\text{M}$), Picrotoxin ($100 \mu\text{M}$) and Gabazine ($5 \mu\text{M}$) to block action potential, NMDA, GABA and GABAA receptors, respectively in whole cell voltage clamp recording configuration. Based on kinetics, the electrophysiological property of mEPSC events such as decay time and frequency, the responses from *Hoxb8* mutants were classified into group 1 and 2. Orange and green bars on the traces represent time periods where no mEPSC activity was detected. Cartoon on the top shows the location of pipette positioning and recording within striatum **h**) mEPSC individual representative events for WT and *Hoxb8* mutants from group 1 and group 2 type of MSN neuronal responses. The amplitude varied among individual events. Small, medium and large amplitude events were recorded and analyzed. **(i-l)** Cumulative probability plot of WT and *Hoxb8* mutants showing rightward shift in the curve for *Hoxb8* mutants for inter-event interval and mEPSC amplitudes for group 1 (**i**, $P=0.002$, $D=0.08375$; $P=0.00029$, $F=13.18906$ for inset; **k**, $P<0.0001$, $D=0.6917$; $P<0.0001$, $F=2654.712$ for inset) and group 2 neurons (**j**, $P<0.0001$, $D=0.7023$; $P<0.0001$, $F=949.241$; **l**, $P<0.0001$, $D=0.2040$; $P<0.0001$, $F=111.279$ for inset). Inset represents bar graph from the same data set. 'n' represents the number of neurons patched per experimental group obtained from 3 WT and 3 *Hoxb8* mutants. At least 100 events were sampled per neuron. Series and input resistance were monitored continuously and neuronal recordings were discarded if these parameter changed by $>20\%$. All experiments were conducted blindly in which the experimenter was unaware of the electrophysiological outcome of different cell types within dorsal striatum. mEPSC's were analyzed using MiniAnalysis Synaptosoft software. One-way ANOVA and Tukey's posthoc test for bar graphs, Kolmogorov-Smirnov test, (i-l). 6 months old WT and *Hoxb8* mutant brain slices were used for the slice electrophysiological experiments.

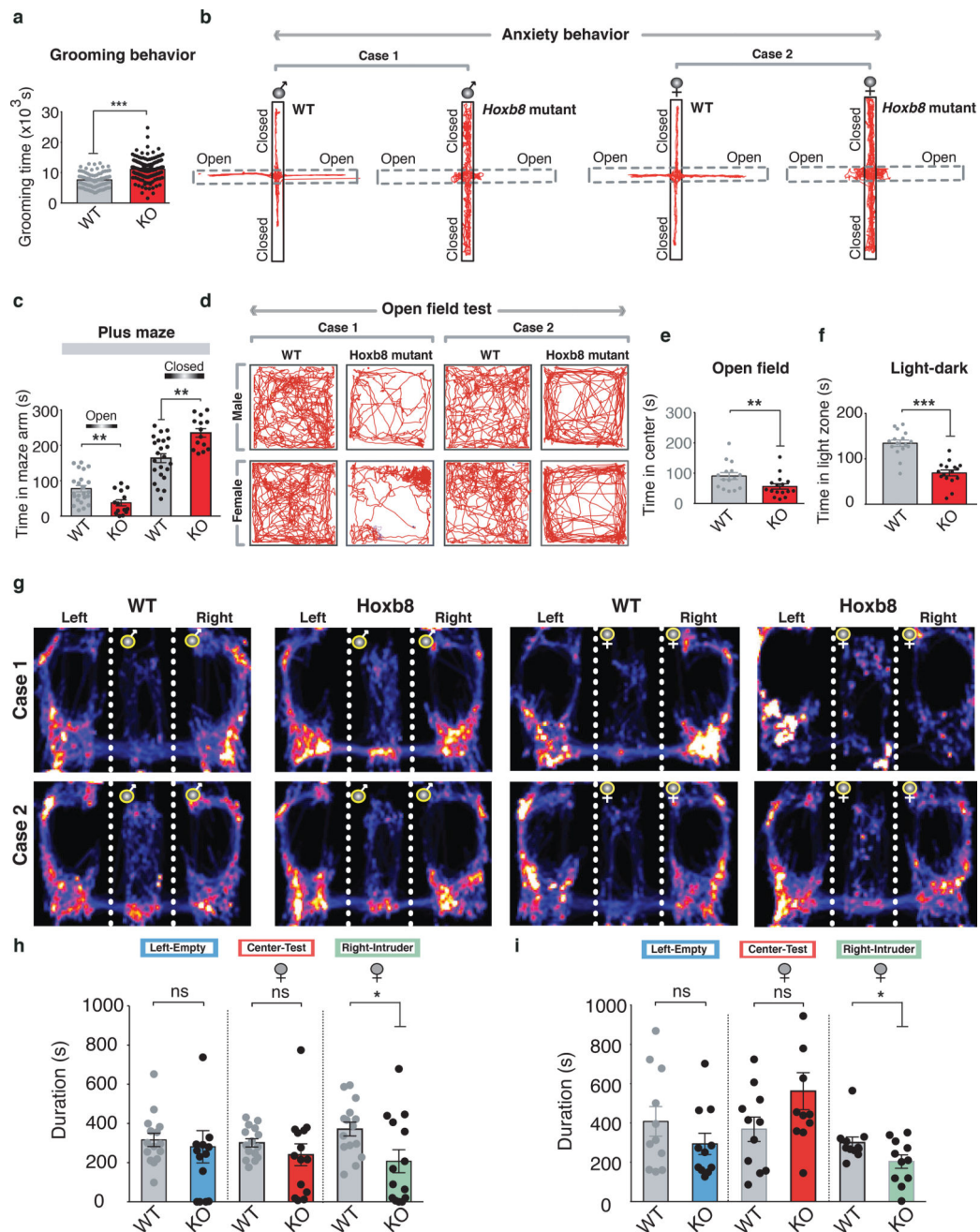


Figure 3. Altered Grooming, anxiety and social behaviors in *Hoxb8* mutants

a) Mutants show increased grooming ($P < 0.0001$, $F = 59.115628$) in 24 hour grooming assay as compared to WT mice (4–12 months old). **b)** Representative track plots of male WT, male mutants, female WT and female mutants in 5 minute elevated plus maze test under ambient light conditions. Note the movement of mutants pertained to closed as compared to open chamber. **c)** *Hoxb8* mutants (6–8 months old) spend reduced time in open ($P = 0.00474$, $F = 9.10139$) and increased time in closed arm ($P = 0.0005$, $F = 14.7216$) (left panel). **d)** Representative track plots of male WT and male mutant (upper panel), female WT and female mutant (lower panel) in the open field test. **e, f)** Mutants (6–8 months old) spend

significantly reduced ($P=0.02369$, $F=5.70155$) time- at the center of the open field in a 30 minute open field test and within the light zone ($P=0.00027$, $F=15.4018$) (right panel) in 5 minute light-dark test (illumination 600 Lx). **g**) Representative heat maps of individual male and female WT and *Hoxb8* mutants (Case 1–2) during three-chambered social interaction assay with an empty left chamber and an intruder in the right chamber (same sex as the test mouse). **h**) Female mutants (6–8 months old) spent significantly reduced time with the intruder mouse in the right chamber ($P=0.1148$, $F=15.40186$ for left chamber non-contact duration; $P=0.3004$, $F=2.6407275$ for the total duration in the center; $P=0.0222$, $F=5.8829406$ for total contact duration with the intruder) in social interaction assay. Data represents Mean \pm SEM, uses one-way ANOVA and Tukey's HSD posthoc test for comparison. ns, not significant $P>0.05$, * $P<0.05$). **i**) Bar graph representation of the comparison of social interaction pattern of female *Hoxb8* mutants and WT mice (6–8 months old) with an empty chamber (left) and a cage-mate (right) ($P=0.0861$, $F=3.27635$ for the non contact duration with the left chamber; $P=0.427$, $F=0.65771$ for total duration in the center; $P=0.0095$, $F=8.325$ for total contact duration with intruder). The cage-mate was of same age and sex as of experimental mice. All bar graph data represents mean \pm SEM. Data comparison, one-way ANOVA and Tukey's HSD posthoc test was used for group comparison. ns, $P>0.05$ not significant, * $P<0.05$, ** $P<0.001$. 4–12 months old mice were used for grooming behavior, 6–8 months old mice for elevated plus maze, open field and social behavioral tests. All test mice were conditioned for 5–15 minutes in specific experimental rooms prior to the experiments. All behavioral experiments were conducted during day light period of the light/dark cycle. All experiments were conducted blindly without the knowledge of experimenter to genotypes.

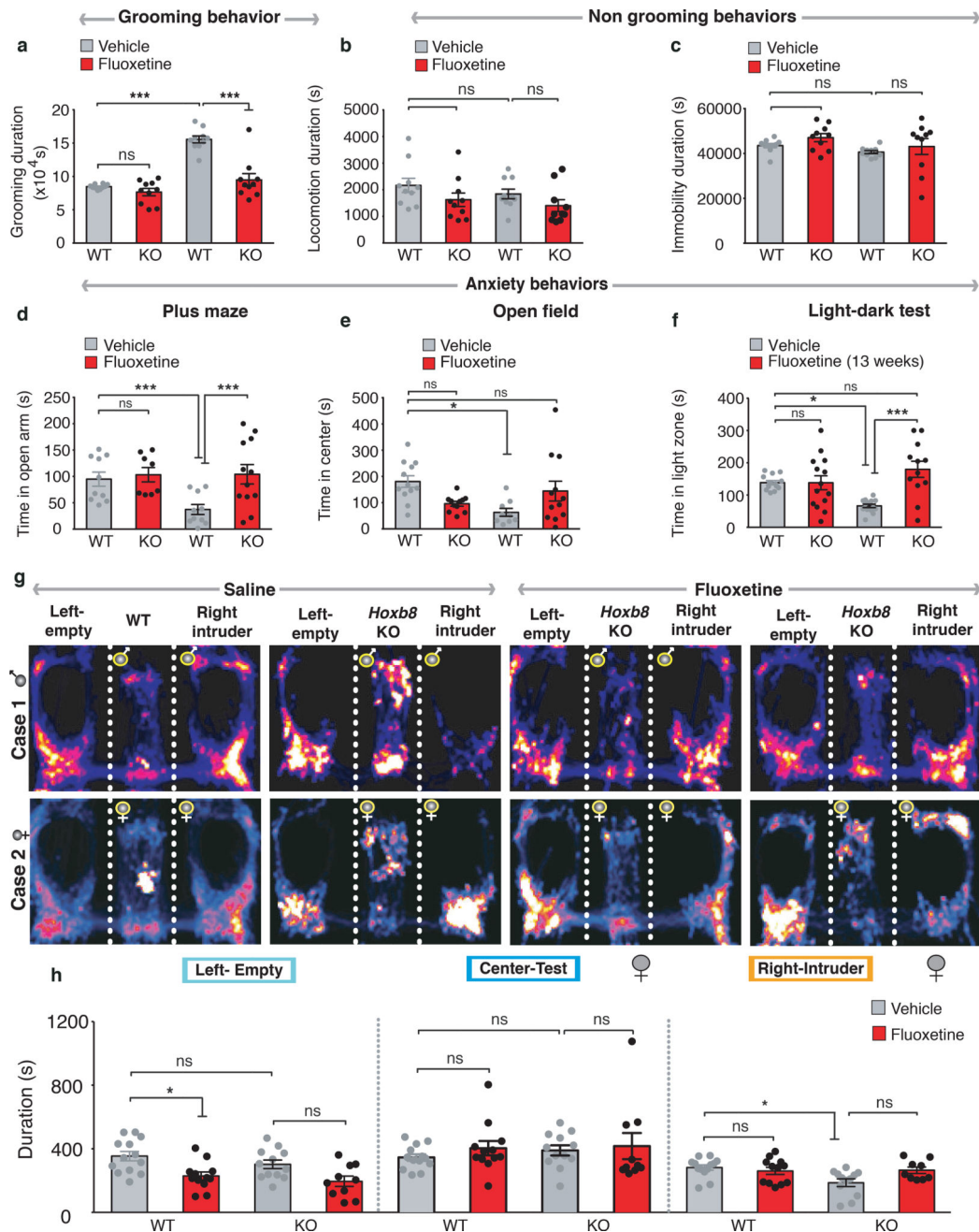


Figure 4. Rescue of grooming, anxiety and social behaviors by chronic fluoxetine treatment

a Rescue of grooming behavior in age- and sex-matched *Hoxb8* mutants (6–12 months) treated with 5 mg/kg fluoxetine in post 5 week treated *Hoxb8* mutants ($P=0.0001$, $F(1, 36)=18.95$ for interaction; $P<0.0001$, $F(1, 36)=32.43$ for drug; $P<0.0001$, $F(1,36)=54.23$ for genotype). **b, c** 5-week treatment did not affect locomotion (**b**, $P=0.8259$, $F(1, 36)=0.04911$ for interaction; $P=0.0434$, $F(1, 36)=4.385$ for drug; $P=0.2486$, $F(1,36)=1.375$ for genotype) and immobility duration (**c**, $P=0.8108$, $F(1, 36)=0.05817$ for interaction; $P=0.1552$, $F(1,36)=2.108$ for drug; $P=0.1074$, $F(1,36)=2.726$ for genotype) significantly in mutants. **d, e** 5-week treated mutants show increased time in the open arm and the center of the open

field. Complete rescue was observed in the plus maze test (d, $P=0.0595$, $F(1,36)=3.788$ for interaction; $P=0.0170$, $F(1,36)=6.261$ for drug; $P=0.0675$, $F(1,36)=3.554$ for genotype) but a partial rescue was noted in the open field test (e, $P=0.0022$, $F(1,36)=10.71$ for interaction; $P=0.9404$, $F(1,36)=0.005653$ for drug; $P=0.1790$, $F(1,36)=1.871$ for genotype) **f**) 13 week treated *Hoxb8* mutants spend more time like WT mice in the light zone as compared to untreated mutants in 5 minute light-dark test ($P=0.0013$, $F(1,49)=11.56$ for interaction; $P=0.0014$, $F(1,49)=11.50$ for drug; $P=0.3651$, $F(1,49)=0.8359$ for genotype). **g**) Representative heat maps of saline- and fluoxetine-treated male and female WT and *Hoxb8* mutants (Case 1–2) during three-chambered social interaction assay with an empty left chamber and an intruder in the right chamber (same sex as test mouse). Rescue of social interaction is more prominent in female *Hoxb8* mutants. **h**) *Hoxb8* mutants show WT-like interaction time with the intruder mouse post two-week fluoxetine treatment in three-chambered social interaction test. The experimental female mouse was placed in the center chamber. The left chamber was left empty and the right chamber consisted of an intruder mouse of same sex as the experimental mouse ($P=0.7438$, $F(1,43)=0.1082$ for interaction; $P=0.0002$, $F(1,43)=16.45$ for drug; $P=0.1429$, $F(1,49)=2.227$ for genotype for the time in left chamber; $P=0.7295$, $F(1,43)=0.1211$ for interaction; $P=0.3615$, $F(1,43)=0.8509$ for drug; $P=0.5411$, $F(1,49)=0.3796$ for genotype for the time in the center chamber; $P=0.1147$, $F(1,43)=2.593$ for interaction; $P=0.5048$, $F(1,43)=0.4523$ for drug; $P=0.0126$, $F(1,49)=6.776$ for genotype for the time in the right chamber). 6–12 months old age-matched WT and *Hoxb8* mutants were used for the experiments.